IEEE Access
Multidisciplinary | Rapid Review | Open Access Journal

Received June 25, 2020, accepted June 29, 2020, date of publication July 3, 2020, date of current version July 15, 2020.

Digital Object Identifier 10.1109/ACCESS.2020.3006825

Vehicular Networks Under Nakagami-*m* Fading Channels: Outage Probability and Ergodic Achievable Rate

YIYANG NI[1,2], (Member, IEEE), YAXUAN LIU[1], (Graduate Student Member, IEEE), QIN WANG[2], (Member, IEEE), YUXI WANG[1], HAITAO ZHAO[2], (Member, IEEE), AND HONGBO ZHU[2], (Member, IEEE)

[1]College of Mathematics and Information Technology, Jiangsu Second Normal University, Nanjing 210013, China
[2]Jiangsu Key Laboratory of Wireless Communications, Nanjing University of Posts and Telecommunications, Nanjing 210003, China

Corresponding authors: Yiyang Ni (niyy@jssnu.edu.cn) and Qin Wang (wangqin@njupt.edu.cn)

This work was supported in part by the National Natural Science Foundation of China under Grant 61701201, Grant 61771252, and Grant 61801238, in part by the Natural Science Foundation of Jiangsu Province under Grant BK20170758 and Grant BK20171444, and in part by the Six Talent Peaks Project in Jiangsu Province.

ABSTRACT Vehicular networks are regarded as an effective solution for the traffic management and road safety. In this paper, the performance of the vehicular networks is investigated under Nakagami-*m* fading channels. The vehicular communication is considered to reuse the same time-frequency with another vehicular communication link, so that both interference and noise produce an effect on each vehicle and infrastructure. Firstly, we derive the closed-form expressions for the outage probability of vehicular links and particularly examine two special cases, that is, high SNR case and weak interference case. For both cases, approximate expressions for outage probability are provided in closed form. Then, we derive lower and upper bounds of ergoidic achievable rate, which are evident to be sufficiently tight to the Monte-Carlo simulated results. Based on these results, we further analyze the high SNR and weak interference scenarios and the asymptotic expressions of ergoidic achievable rate are also presented. All the analytical results are applicable for arbitrary locations, transmit power, as well as channel parameters. Finally, we propose the power optimization which aims at maximizing the ergodic achievable rate and guaranteeing the outage performance. Numerical results validate our analytical results via Monte Carlo simulations.

INDEX TERMS Ergodic achievable rate, Nakagami-*m* fading, outage probability, vehicular networks.

I. INTRODUCTION

In recent years,with the seamless increase of vehicles, come along a series of critical global problems including heavy traffic, traffic accidents, as well as air pollution caused by traffic congestion [1]. According to statistics, more than 1.3 million people were dead worldwide in traffic accidents each year [2]. As a broad consensus, vehicular networks are regarded as an effective solution to these issues. The traffic efficiency and safety can be effectively enhanced by the potential of the vehicular networks, which can enable awareness of neighboring vehicles through transmitting the real-time messages to both drivers and passengers [3]–[6].

The associate editor coordinating the review of this manuscript and approving it for publication was Young Jin Chun.

Due to these benefits, great efforts have been spent on vehicle-to-infrastructure (V2I) communication networks and vehicle-to-vehicle (V2V) communication [7]–[9]. To meet the demand for the vehicular communication, many works focus on the resource allocation schemes of vehicular networks [10]–[15]. A joint resource allocation algorithm was presented to minimize the tracking error while guaranteeing the reliability of the vehicular networks [10]. The resource optimization schemes were proposed to improve the resource utilization efficiency of the vehicular networks overlay device-to-device link, where the resource of D2D link was assumed to be orthogonal to the cellular link [11]. The resource management strategies for the relay-assisted V2V system was investigated in [12] where the road side units (RSUs) were considered as relay nodes. In order to maximize the overall packets receive ratio

performance, a resource allocation mechanism is introduced with non-orthogonal multiple access based V2V system [13]. An optimization method was proposed to allocate the spectrum resource by taking vehicle's priority level and spectrum availability into account for LTE V2V communication [14]. In order to maximize the throughput of vehicular communication network, a reliability and latency aware resource allocation scheme was provided in [15].

The system performance under Nakagami-*m* channel has also drawn much attention. The closed-form expressions for both outage probability and throughput were presented in a single hop wireless powered communication system [32]. The interference is characterized in a homogenous Poisson field of static interferers under Nakagami-*m*, yet the factor noise is left out in the consideration [35]. The orthogonal frequency division multiplexing based DF relay node over a Nakagami fading channels was discussed and the corresponding signal-to-interference-plus-noise ratio (SINR) was derived [36]. In [37], researchers investigated the downlink NOMA networks over Nakagami-m fading channels. The closed-form expressions for the outage probability and intercept probability were obtained and the approximations for high SNR scenario were analyzed. The outage probability and throughput were derived with analytical approximate closed-form expressions for the hybrid satellite/unnamed aerial vehicle (UAV) NOMA networks [38]. The high SNR approximation and diversity orders were explored and an optimal location scheme for the UVA was provided.

Despite the seamless increase in the number of vehicles in recent years, the current researches are lacking in the practical physical layer assumptions. The performance analysis for the vehicular networks has attracted wide attention over the past few years. The performance and reliability of vehicle communication for the safety-critical data broadcasting with different priorities were analyzed in [16], [17]. The authors in [18], [19] investigated the outage performance of vehicular communication via a direct link reusing the cellular uplink resources. Specifically, the urban area modeled as a grid-link street layout was considered in [18]. The closed-form expressions for the performance of vehicular Ad-hoc networks were derived with line of sight (LOS) and single Rayleigh fading channel respectively [20]. The performance of cluster-based heterogenous vehicular networks is analyzed based on a Markov queuing model [21]. Note that the Rayleigh scattering channel was considered in [18]–[21]. Researchers evaluated the performance of LTE-V2D system for both LOS and NLOS cases based on an intersection simulation scenario [22]. Authors in [23] focus on the vehicular communication in 5G small-cell networks, and derived the cooperative probability, as well as coverage probability where the small-cell base stations follow Poisson point process distribution. The throughput of V2I and V2V networks was analyzed in [24] where a closed-form expression was presented under simple channel model. Authors considered the AF-assisted vehicular networks over Nakagami-m fading channels and provided the lower bounds of outage performance [25]. The performance of NOMA SWIPT amplify-and-forward networks under Weibull fading channels was analyzed in [26] where the lower bound for the outage probability, as well as the throughput were provided with closed form. Authors in [27] investigated the performance of an inter-vehicle communication system, and the exact closed-form probability and symbol error were derived. However, obtained based on Meijer's G function, the results in this paper is actually not a closed-form expression in its real sense. Authors in [28] investigated the connectivity probability in the presence of Nakagami fading channel and presented closed-form expression for the connectivity probability. However, the expression is a combination of integral identities and the noise at each user is ignored. In [29], authors focused on the network connectivity probability of one dimensional linear vehicular ad hoc network under Nakagami fading channel. A closed-form expression for the network connectivity probability was obtained with Meijer's G function. However, the influence of the interference was not considered.

Motivated by the above literatures, in this paper, we investigate the system performance of vehicular networks under Nakagami-*m* fading channels which is a versatile fading model compared to the Rayleigh fading channel. We assume that the V2V and V2I communicate by sharing the same time-frequency with the other vehicular link which brings the interference. We first derive the probability density function (PDF) of SINR with closed-form expression. Then we provide the closed form expressions for outage probability of each link where the interference and noise are both considered at each node. Based on the results, we discuss two special scenarios including high SNR case and weak interference case and the simpler approximations are obtained. Based on theoretical analyses, the diversity order of outage probability is obtained. Furthermore, we present the tight bounds for the ergodic achievable rate with closed-form expressions. Similarly, two special cases are investigated and the corresponding approximate closed-form expressions are also proposed. Based on the theoretical analyses for the ergodic achievable rate, we discuss the high-SNR slope. The analytical results demonstrate how the location of vehicle, the wireless channel, and the transmit power affect the system performance. Finally, we give a power allocation scheme to enhance the ergodic achievable rate while the outage performance is guaranteed. Note that all the analysis in our paper apply for arbitrary transmit power, channel parameters and noise, as well as random placement of the vehicle.

The paper structure is as follows: Section II describes the vehicular communication system which shares the same time-frequency resource. In Section III, the closed-form expressions for outage probability are derived and the special cases are discussed. We provide the tight bounds for the ergodic achievable rate with closed-form expressions, as well as, the approximations for the two special cases in Section IV. A power allocation scheme is presented to raise the ergodic achievable rate while guaranteeing the outage performance

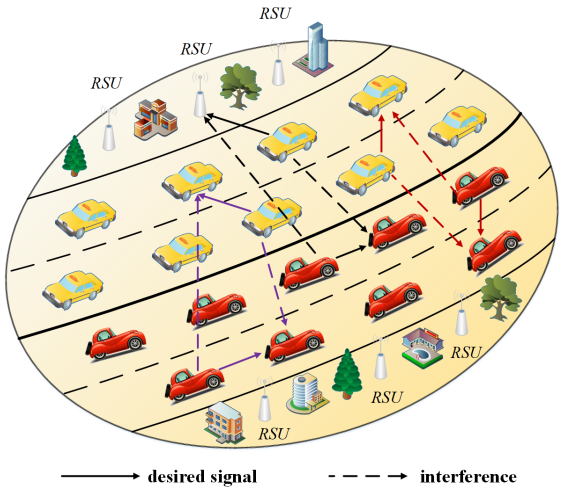

FIGURE 1. The vehicular network where the vehicles and infrastructures communicate by sharing the same time-frequency resources.

in Section IV. A set of numerical results in Section V corroborate our analytical results. Finally, Section VI concludes the paper.

It is convenient to define the following notations: The symbol $\triangleq$ refers to the definition whereas $|\cdot|$ represents the absolute value of a scalar. We use $\Pr(\cdot)$ to denote the probability, while $\Gamma(\cdot)$ stands for the Gamma function. $f_X(\cdot)$ represents the probability density function (PDF) and $F_X(\cdot)$ returns cumulative distribution function (CDF). Finally, $E[\cdot]$ indicates the expectation operator.

II. SYSTEM MODEL

In this paper, we consider the vehicular communications network where there exist multiple vehicles requiring high-capacity V2I communications, and multiple pairs of vehicles engaged in local V2V data exchanging in the form of D2D communications. All the vehicles are capable of doing both V2I and V2V communication simultaneously. The whole uplink frequency bandwidth is divided into F subbands, we assume that only a single pair of V2V is supported via resource reuse with a V2I pair in each subcarrier/subband in the form of D2D communication. For the vehicular networks with multiple V2V pairs, the system assigns each subcarrier to at most one V2V pair and then performs transmission design for the V2I link and assigned V2V link. Without loss of generality, in the rest of our paper, we can simplify the model and focus on a system where the infrastructure serves a single vehicle with a co-existing V2V pair. Unfortunately, for the general vehicular communication system with direct links, the interference is more complicated. As depicted in Fig. 1, the vehicles in proximity communicate with each other by reusing the same frequency with another communication link. In such a vehicular network, the V2V pair transmitter V_T sends message to the receiver vehicle V_R. At the same transmission time duration, the V2I pair transmitter V_1 communicates with RSU. We assume the transmit power of node k as P_k $(k = T, R, 1, U)$,[1] and set s_k as the normalized transmit symbols for node k with $E\left[|s_k|^2\right] = 1$. The channel coefficients of the links are considered to follow independent and non-identically distributed (i. n. d) Nakagami-*m* distribution. Hence, the channel fading power gain can be written as

$$f_{|h_{kq}|^2}(\beta_k) = \left(\frac{m_k}{\Omega_k}\right)^{m_k} \frac{\beta_k^{m_k-1}}{\Gamma(m_k)} \exp\left(-\frac{m_k\beta_k}{\Omega_k}\right) \tag{1}$$

where h_{kq} $(q = R, T, 1, U; q \neq k)$ represents the channel fading coefficient, m_k denotes the fading parameter which is assumed to be a positive integer, $\Omega_k = E\left[\left|h_{kq}^2\right|\right]$ denotes the mean power, while $\Gamma(\cdot)$ is gamma function. We assume all the nodes are affected by the additive white Gaussian noise n_k with zero-mean and variance of N_0. We characterize the path loss factors as $L_{kq} = \left(d_0/d_{kq}\right)^{\alpha}$ where α is the path-loss exponent, d_0 stands for the reference distance and d_{kq} denotes the distance between node k and q. Because the V2V links share the same time-frequency resource, the two links interfere with each other. Then, the received signal at V_R can be expressed by

$$y_R = \sqrt{P_T L_{TR}} h_{TR} s_T + \sqrt{P_1 L_{1R}} h_{1R} s_1 + n_R \tag{2}$$

while the signal obtained by RSU is given by

$$y_U = \sqrt{P_1 L_{1U}} h_{1U} s_1 + \sqrt{P_{TU} L_{TU}} h_{TU} s_T + n_U. \tag{3}$$

Based on the expressions in (2) and (3), we can write the SINR at V_R and RSU respectively as

$$\gamma_R = \frac{P_T L_{TR} |h_{TR}|^2}{P_1 L_{1R} |h_{1R}|^2 + N_0} \tag{4}$$

and

$$\gamma_U = \frac{P_1 L_{1U} |h_{1U}|^2}{P_T L_{TU} |h_{TU}|^2 + N_0}. \tag{5}$$

The outage probability is considered as a crucial quality of service metric, which can be calculated by integrating the PDF of γ from 0 to an acceptable threshold γ_{th}. Hence, the outage probability of $k - q$ link can be obtained by

$$\Pr_{kq}^{out} = \Pr\left(\gamma_{kq} \leq \gamma_{th}\right) = \int_0^{\gamma_{th}} f\left(\gamma_{kq}\right) d\gamma_{kq} \tag{6}$$

where $f\left(\gamma_{kq}\right)$ is the PDF of the received SINR of $k - q$ link. In addition, we can write the ergodic achievable rate as follow

$$R_{kq} = E\left[\log_2\left(1 + \gamma_{kq}\right)\right]. \tag{7}$$

Prior to starting our investigation of the system performance, a new key lemma is provided which will be used in the subsequent analysis.

Lemma 1: Given three constants μ, η, ξ satisfying $Re[\mu] > 0, Re[\eta] > 0, Re[\xi] > 0$, and two positive integers $n_1, n_2 \in N$, for the function

$$I(\mu, \eta, \xi; n_1, n_2) = \int_{\xi}^{+\infty} \frac{x^{n_1} \exp(-\mu x)}{(x + \eta)^{n_2}} dx \tag{8}$$

[1]Note that T stands for V_T, R represents V_R, and 1, U respectively refer to the V_1 and RSU.

we have

$$I(\mu,\eta,\xi;n_1,n_2) = \begin{cases} exp(\mu\eta)\left[\sum_{j=0}^{n_2} C_{n_1}^{j}\frac{(-\eta)^{n_1-j}}{(\xi+\eta)^{n_2-j-1}}E_{n_2-j}(\mu(\eta+\xi)) + \sum_{j=n_2+1}^{n_1} C_{n_1}^{j}(-\eta)^{n_1-j}\mu^{n_2-j-1}\Gamma(j-n_2+1,\mu(\eta+\xi))\right], & n_1 > n_2 \\ exp(\mu\eta)\sum_{j=0}^{n_1} C_{n_1}^{j}\frac{(-\eta)^{n_1-j}}{(\xi+\eta)^{n_2-j-1}}E_{n_2-j}(\mu(\xi+\eta)), & n_1 \le n_2 \end{cases} \quad (9)$$

where $E_n(p)$ is Exponential Integral and is expressed by

$$E_n(p) = \frac{(-p)^{n-1}}{(n-1)!}[-\ln p + \psi(n)] - \sum_{m=0}^{\infty}\frac{(-p)^m}{(m-n+1)\,m!} \quad (10)$$

with

$$\begin{cases} \psi(1) = -\gamma \\ \psi(n) = -\gamma + \sum_{m=1}^{n-1}\frac{1}{m} \quad n>1 \end{cases} \quad (11)$$

where $\gamma \approx 0.577$ is Euler's constant.

Proof: See Appendix A. □

Here, *Lemma 1* provides a simple and computationally efficient expression with closed form, which only includes several elementary functions. It is also worth noting that $I(\cdot,\cdot,\cdot;\cdot,\cdot)$ is a monotonically decreasing function with μ, η and ξ. Having established the results in *Lemma 1*, we are now ready to investigate the outage probability and ergodic achievable rate for the vehicular networks under Nakagami-m fading channel. Note that the interference expressions for links $V_T - V_R$ and $V_1 - RSU$ are similar, except that the coefficients are different. Therefore, to find either the outage probability or the ergodic achievable rate, we only need to find the performance of one link, and then the other one can be naturally obtained in the same manner.

III. OUTAGE PROBABILITY ANALYSIS

In this subsection, we first derive the closed-form expression for the PDF of SINR. Then we obtain the outage probability of both $V_T - V_R$ and V_1-RSU links with closed-form solution. Subsequently, we discuss two special scenarios involving high SNR and weak interference, for each special scenario, we give the approximations with simple closed-form expressions.

A. EXACT OUTAGE PROBABILITY

For the sake of convenience, we define the following notations, $\sigma_1 = P_T L_{TR}$, $\sigma_2 = P_1 L_{1R}$, $U = \sigma_1|h_{TR}|^2$ and $V = \sigma_2|h_{1R}|^2 + N_0$ and then we have

$$f_U(u) = \frac{1}{\sigma_1}f\left(\frac{u}{\sigma_1}\right) \quad (12)$$

and

$$f_V(v) = \frac{1}{\sigma_2}f\left(\frac{v-N_0}{\sigma_2}\right). \quad (13)$$

According to the expression in (2), we further obtain the PDF of γ_R as follows

$$f_{\gamma_R}(w) = \int_{-\infty}^{+\infty}|v|\cdot f_{UV}(wv,v)dv \quad (14)$$

where $f_{UV}(\cdot)$ is joint probability density function. Since U, V are independent, $f_{\gamma_R}(w)$ is given by

$$f_{\gamma_R}(w) = \int_{N_0}^{+\infty} v\cdot f_U(wv)\cdot f_V(v)\,dv. \quad (15)$$

Submitting (12) and (13) into (15), we have

$$f_{\gamma_R}(w) = \prod_{l=1}^{2}\left(\frac{m_l}{\Omega_l}\right)^{m_l}\frac{1}{\Gamma(m_l)} \times \int_{N_0}^{+\infty} v\frac{1}{\sigma_1}\left(\frac{wv}{\sigma_1}\right)^{m_1-1}\exp\left(-\frac{m_1 wv}{\Omega_1\sigma_1}\right) \times\frac{1}{\sigma_2}\left(\frac{v-N_0}{v}\right)^{m_2-1}\exp\left(-\frac{m_2(v-N_0)}{\Omega_2\sigma_2}\right)dv \quad (16)$$

where m_1 stands for the fading parameter of h_{TR} while m_2 refers to the fading parameter of h_{1R}. Let $v \leftarrow v - N_0$, after some manipulations, (16) can be transformed into

$$f_{\gamma_R}(w) = \prod_{l=1}^{2}\left(\frac{m_l}{\sigma_l\Omega_l}\right)^{m_l}\frac{1}{\Gamma(m_l)}w^{m_1-1} \times\exp\left(-\frac{m_1N_0w}{\Omega_1\sigma_1}\right)\int_{0}^{+\infty}(v+N_0)^{m_1}v^{m_2-1} \times\exp\left(-\frac{m_1}{\Omega_1\sigma_1}\left(w+\frac{m_2\Omega_1\sigma_1}{m_1\Omega_2\sigma_2}\right)v\right)dv. \quad (17)$$

Utilizing Eq.(3.151.3) in [41], the PDF of γ_R is written as

$$f_{\gamma_R}(w) = \prod_{l=1}^{2}\left(\frac{m_l}{\sigma_l\Omega_l}\right)^{m_l}\frac{1}{\Gamma(m_l)}\times w^{m_1-1} \times\exp\left(-\frac{m_1N_0w}{\Omega_1\sigma_1}\right) \times\sum_{i=0}^{m_1}\frac{C_{m_1}^{i}N_0^{m_1-i}\left(\frac{\Omega_1\sigma_1}{m_1}\right)^{m_2+i}}{\left(w+\frac{m_2\Omega_1\sigma_1}{m_1\Omega_2\sigma_2}\right)^{m_2+i}}\Gamma(m_2+i) \quad (18)$$

where $C_{m_1}^{i}$ is the m_1-combination of i. Having obtained the pdf of γ_R, we now derive the main results as follows.

Theorem 1: When each vehicle and RSU are influenced by both interference and noise, the outage probability of V2V link under independent Nakagami-m fading is given by

$$\begin{aligned}\Pr_R(\gamma_{th}) = 1 - \prod_{l=1}^{2}\left(\frac{m_l}{\sigma_l\Omega_l}\right)^{m_l}\frac{1}{\Gamma(m_l)} \\ \times \sum_{i=0}^{m_1} C_{m_1}^{i} N_0^{m_1-i}\left(\frac{\Omega_1\sigma_1}{m_1}\right)^{m_2+i}\Gamma(m_2+i) \\ \times I\left(\frac{m_1N_0}{\Omega_1\sigma_1}, \frac{m_2\Omega_1\sigma_1}{m_1\Omega_2\sigma_2}, \gamma_{th}; m_1-1, m_2+i\right) \quad (19)\end{aligned}$$

where $I(\cdot,\cdot,\cdot;\cdot,\cdot)$ is shown in *Lemma 1*.

Proof: According to the definition of outage probability in (6), we have

$$\begin{aligned}\Pr(\gamma_R \le \gamma_{th}) &= 1 - \Pr(\gamma_R > \gamma_{th}) \\ &= 1 - \int_{\gamma_{th}}^{+\infty} f_{\gamma_R}(w)dw. \quad (20)\end{aligned}$$

Submitting the PDF of SINR into (20), we obtain the following formula

$$\begin{aligned}\int_{\gamma_{th}}^{+\infty} f_{\gamma_R}(w)dw = \prod_{l=1}^{2}\left(\frac{m_l}{\sigma_l\Omega_l}\right)^{m_l}\frac{1}{\Gamma(m_l)} \\ \times \sum_{i=0}^{m_1} C_{m_1}^{i} N_0^{m-i}\left(\frac{\Omega_1\sigma_1}{m_1}\right)^{m_2+i}\Gamma(m_2+i) \\ \times \int_{\gamma_{th}}^{+\infty} \frac{w^{m_1-1}}{\left(w+\frac{m_2\Omega_1\sigma_1}{m_1\Omega_2\sigma_2}\right)^{m_2+i}}\exp\left(-\frac{m_1N_0w}{\Omega_1\sigma_1}\right)dw. \quad (21)\end{aligned}$$

Then the equation (19) in *Theorem 1* can be easily evaluated based on the results in *Lemma 1*. □

Note that the outage probability of V1-RSU link can be obtained in exactly the same way. It is obvious that the result in (19) relies on several system parameters including the desired signal power σ_1 from V_T, the interference signal power σ_2 from V2V link, the noise N_0 and the fading parameters for desired V2V channel and interfered channel. The results in *Theorem 1* gives the exact outage probability of each V2V link or V2I link which applies for arbitrary transmit power, noise, distance between the vehicles and infrastructures, as well as channel parameters. Note that the expression in *Theorem 1* is presented with closed-form including standard functions which can be evaluated computationally and efficiently. In addition, a special case was proposed in [42] where $m_1 = m_2$ is assumed.

Corollary 1: For the Rayleigh fading case, the outage probability is presented as

$$\Pr^{Ray} = 1 - \frac{\sigma_1}{\sigma_2\gamma_{th}+\sigma_1}\exp\left(-\frac{N_0}{\sigma_1}\gamma_{th}\right). \quad (22)$$

Proof: In equation (19), we set $m_1 = m_2 = 1$ and the $I(\cdot,\cdot,\cdot;\cdot,\cdot)$ can be simplified as

$$\begin{aligned}&I\left(\frac{N_0}{\sigma_1}, \frac{\sigma_1}{\sigma_2}, \gamma_{th}, 0, 1+i\right) \\ &= \frac{1}{(\gamma_{th}+\sigma_1/\sigma_2)^i}\exp\left(\frac{N_0}{\sigma_2}\right)E_{1+i}\left(\frac{N_0\gamma_{th}}{\sigma_1}+\frac{N_0}{\sigma_2}\right). \quad (23)\end{aligned}$$

The expression of outage probability in Rayleigh fading case can be written as

$$\begin{aligned}\Pr^{Ray} = 1 - \frac{N_0}{\sigma_2}\exp\left(\frac{N_0}{\sigma_2}\right)E_1\left(\frac{N_0\gamma_{th}}{\sigma_1}+\frac{N_0}{\sigma_2}\right) \\ + \frac{\sigma_1}{\gamma_{th}+\sigma_1}\exp\left(\frac{N_0}{\sigma_2}\right)E_2\left(\frac{N_0\gamma_{th}}{\sigma_1}+\frac{N_0}{\sigma_2}\right) \quad (24)\end{aligned}$$

considering that the $E_n(p)$ function meets the following recursive formula

$$nE_{n+1}(p) = e^{-p} - pE_n(p). \quad (25)$$

Set $n = 1$, and then we can acquire a simpler form of the equation (24) in *Corollary* 1. □

We now examine two scenarios of *Theorem 1* where the expressions will reduce to simpler forms.

B. HIGH SNR CASE

Corollary 2: For the high SNR case, the outage probability reduces to

$$\begin{aligned}\Pr^{HS} &= \Pr(\gamma_R \le \gamma_{th})|_{i=m_1, N_0\to 0} \\ &\approx 1 - \left(\frac{m_2\Omega_1\sigma_1}{m_1\Omega_2\sigma_2}\right)^{m_2}\frac{\Gamma(m_1+m_2)}{\Gamma(m_1)\Gamma(m_2)} \\ &\quad \times I\left(0, \frac{m_2\Omega_1\sigma_1}{m_1\Omega_2\sigma_2}, \gamma_{th}; m_1-1, m_1+m_2\right). \quad (26)\end{aligned}$$

Proof: In this case, the additive noise can be ignored so we have $P_i/N_0 \to \infty$. According to the expression in *Theorem 1*, it's obvious that $\Pr \neq 0$ only when $i = m_1$. Therefore, the outage probability for high SNR case in *Corollary 2* is trivially obtained by taking $N_0 \to 0$ and $i = m_1$ into (19). □

Thus, it is easily conceivable that the expression for high SNR case is much simpler and the outage performance is enhanced as the desired signal power from V_T decreases. We can also find that a ceiling is excited in the high SNR levels when the transmit power of each vehicle is fixed, since the outage performance is independent of SNR but only depends on the signal-to-interference ratio(SIR). The approximation in (26) will be shown converging to the exact outage probability curves for high SNR regime in Fig. 3.

The diversity order usually aims to describe how fast the outage probability decreases with the transmitting SNR. Accordingly, the diversity order can be defined as [39]

$$d = -\lim_{\rho\to\infty}\frac{\log(P^{\infty}(\rho))}{\log\rho} \quad (27)$$

where $P^{\infty}(\rho)$ refers to the asymptotic outage probability for high SNR case. Since the expression in *Corollary 2* is independent of SNR, we can easily get the diversity order for the outage probability.

Remark:1 By substituting the result in *Corollary 2* into (27), the diversity order is equal to *zero*. This is due to the fact that the received interference form the communication link which shares the same time-frequency resources.

C. WEAK INTERFERENCE CASE

Corollary 3: For the weak interference case, the outage probability reduces to

$$\Pr^{WI}(\gamma_R \le \gamma_{th}) = \frac{1}{\Gamma(m_1)}\gamma\left(m_1, \frac{m_1\gamma_{th}N_0}{\sigma_1\Omega_1}\right) \tag{28}$$

where $\gamma(\cdot,\cdot)$ is lower incomplete gamma function, defined as

$$\gamma(n,z) = (n-1)! - \exp(-z)\sum_{k=0}^{n-1}\frac{(n-1)!}{k!}z^k. \tag{29}$$

Proof: When the V2V link and V2I link sharing the same time-frequency is far away from each other, the interference between two links becomes negligible. Under such circumstances, the received SINR is expressed by $\gamma_R^{WI} \approx \sigma_1|h_1|^2/N_0$. Similar to the previous derivation, we can easily present the approximate expression for the weak interference case in *Corollary 3*. □

Again, we see a simpler expression for the weak interference case. Since the received signal power decreased exponentially with the distance between two links, it results in the disappearance of the received interference signal power in (28). According to the result in (28), we clearly see that when the threshold γ_{th} is fixed, the dominating factor on the outage probability is the received SNR and the noise. This approximation is verified later in Fig. 4.

IV. ERGODIC ACHIEVABLE RATE

In this subsection, we first give the exact expression for the ergodic achievable rate of V2V link, and then we present the tight bounds, which admit simpler expressions with closed form. Furthermore, we also examine high SNR case and weak interference case, and approximate closed-form expressions for each case are provided, respectively. Having established the pdf of γ_{th} in (1), we can write the ergodic achievable rate of V2V link as follows

$$\begin{aligned} R_R &= E\left[\log_2(1+\gamma_R)\right] \\ &= \int_0^{+\infty}\log_2(1+w)\times\prod_{l=1}^{2}\left(\frac{m_l}{\sigma_l\Omega_l}\right)^{m_l} \\ &\quad\times\frac{1}{\Gamma(m_l)}w^{m_1-1}\exp\left(-\frac{m_1N_0w}{\Omega_1\sigma_1}\right) \\ &\quad\times\sum_{i=0}^{m_1}\frac{C_m^iN_0^{m-i}\left(\frac{\Omega_1\sigma_1}{m_1}\right)^{m_2+i}}{\left(w+\frac{m_2\Omega_1\sigma_1}{m_1\Omega_2\sigma_2}\right)^{m_2+i}}\Gamma(m_2+i)dw. \end{aligned} \tag{30}$$

A. TIGHT BOUND ANALYSIS

Note that the computation of the exact expression for the ergodic achievable rate in (30) is complicated, although the integral in (30) can be evaluated numerically. Consequently, deriving tight closed-form upper and lower bounds for the ergodic achievable rate with closed-form expressions is important and efficient. Here, we propose new upper and lower bounds on the ergodic achievable, as is shown in *Theorem 2*.

Theorem 2: When each vehicle and infrastructure are influenced by both interference and noise, the ergodic achievable rate of V2V link under independent Nakagami-*m* fading is bounded by

$$R_{R,lo} \le R_R \le R_{R,up} \tag{31}$$

where

$$R_{R,lo} = \log_2\left(1+\frac{1}{\Phi I\left(\frac{m_1N_0}{\Omega_1\sigma_1}, \frac{m_2\Omega_1\sigma_1}{m_1\Omega_2\sigma_2}, 0; m_1-2, m_2+i\right)}\right) \tag{32}$$

and

$$R_{R,up} = \log_2\left(1+\Phi I\left(\frac{m_1N_0}{\Omega_1\sigma_1}, \frac{m_2\Omega_1\sigma_1}{m_1\Omega_2\sigma_2}, 0; m_1, m_2+i\right)\right) \tag{33}$$

with

$$\begin{aligned} \Phi &= \prod_{l=1}^{2}\left(\frac{m_l}{\sigma_l\Omega_l}\right)^{m_l}\frac{1}{\Gamma(m_l)} \\ &\quad\times\sum_{i=0}^{m_1}C_m^iN_0^{m-i}\left(\frac{\Omega_1\sigma_1}{m_1}\right)^{m_2+i}\Gamma(m_2+i). \end{aligned} \tag{34}$$

Proof: See Appendix B. □

It is important to note that *Theorem 2* gives the closed-form bounds for the ergodic achievable rate for arbitrary transmit power, as well as location of each vehicles and infrastructures. Our results in *Theorem 2* are computationally efficient, including only several elementary functions. Moreover, the interference and noise are both considered in the derivation. The new bounds proposed in (31) will be compared with Monte Carlo results and a perfect agreement will be shown in Section V. Two special scenarios will also be discussed hereafter to demonstrate more insightful characterizations.

B. HIGH SNR CASE

Corollary 4: For the high SNR case, the ergodic achievable rate bounds reduces to

$$R_{R,lo}^{HS} \le R_R^{HS} \le R_{R,up}^{HS} \tag{35}$$

where

$$\begin{aligned} R_{R,lo}^{HS} &= R_{R,lo}^{HS}|_{i=m_1,N_0\to0} \\ &= \log_2\left(1+\frac{m_2\Omega_1\sigma_1\Gamma(m_1)\Gamma(m_2)}{\psi_{lo}}\right) \end{aligned} \tag{36}$$

and

$$\begin{aligned} R_{R,up}^{HS} &= R_{R,up}^{HS}|_{i=m_1,N_0\to0} \\ &= \log_2(1+\psi_{up}) \end{aligned} \tag{37}$$

with

$$\psi_{lo} = m_1\Omega_2\sigma_2\Gamma(m_1+m_2) \times \sum_{j=0}^{m_1-2} C_{m_1-2}^{j}(-1)^{m_1-2-j}E_{m_1+m_2-j}\left(0^+\right) \quad (38)$$

and

$$\psi_{up} = \frac{m_2\Omega_1\sigma_1}{m_1\Omega_2\sigma_2}\frac{\Gamma(m_1+m_2)}{\Gamma(m_1)\Gamma(m_2)} \times \sum_{j=0}^{m_1} C_{m_1}^{j}(-1)^{m_1-j}E_{m_1+m_2-j}\left(0^+\right). \quad (39)$$

Proof: For $N_0 \to 0$, as observed from the expressions of upper and lower bounds, it is solvable only when $i = m_1$. Then it yields the results in *Corollary 4*. □

It is obvious that the expressions in *Corollary 4* are simpler than the exact ergodic achievable rate given for this regime in *Theorem 2*. We can explicitly find that the results in *Corollary 4* only rely on the desired signal power, interference signal power and channel parameters which imply an upper limit existed in the approximations.

The high SNR slope is selected to capture the diversification of ergodic rate with the transmitting SNR, which is expressed by [40]

$$s = \lim_{\rho\to\infty}\frac{R^{\infty}(\rho)}{\log\rho} \quad (40)$$

where $R^{\infty}(\rho)$ refers to the asymptotic ergodic achievable rate for high SNR regime.

Remark:2 By substituting the result in *Corollary 4* into (40), we have

$$0 = \lim_{\rho\to\infty}\frac{R_{R,lo}^{\infty}(\rho)}{\log\rho} \le s \le \lim_{\rho\to\infty}\frac{R_{R,up}^{\infty}(\rho)}{\log\rho} = 0 \quad (41)$$

Therefore, due to the influence of received interference, the high SNR slope is equal to *zero*.

C. WEAK INTERFERENCE CASE

Corollary 5: For the weak interference case, the ergodic achievable rate bounds reduces to

$$R_{R,lo}^{WI} \le R_R^{WI} \le R_{R,up}^{WI} \quad (42)$$

where

$$R_{R,lo}^{WI} = \log_2\left(1+\frac{\Omega_1\sigma_1(m_1-1)}{m_1N_0}\right) \quad (43)$$

and

$$R_{R,up}^{WI} = \log_2\left(1+\frac{\Omega_1\sigma_1}{N_0}\right). \quad (44)$$

Proof: Based on the analysis in Section III-C, we have $\sigma_2 \to 0$. Based on the aforementioned analysis, the upper and lower bounds in *Corollary 5* can be easily arrived. □

Clearly, results in *Corollary 5* provide extraordinary concise expressions for the ergodic achievable rate bounds under the scenario where the interference link is far away from the desired link. Interestingly, the asymptotic upper bound is only related to the received signal power and the noise. In addition, it could be seen from equations (43) and (44) that when the value of m_1 goes to infinity, the two equations will eventually aggregate. That is, the larger the value of m is, the closer upper and lower bounds and the more accurate the solution is.

D. POWER ALLOCATION

We now focus on power allocation to maximize the ergodic achievable rate of each link, with guarantee on the outage probability performance. In the previous discussion, the transmit power is considered unchanged. However, in a more realistic scenario, the total transmit power constraint should be considered, that is $P_T + P_1 = P_{Total}$. In order to investigate the power allocation scheme, we assume the transmit power of V_T, V_1 as φP_{Total} and $(1-\varphi)P_{Total}$, respectively. The problem is formulated as

$$\begin{aligned} &\max_{\varphi}\ [R_R(\varphi), R_U(1-\varphi)]^T \\ &s.t.\ \varphi \in [0,1] \\ &\quad Pr_R(\varphi) \le p_R \\ &\quad Pr_U(1-\varphi) \le p_U \end{aligned} \quad (45)$$

where $R_U(1-\varphi)$ refers to the ergodic achievable rate of V_1-RSU link.

In order to reduce the difficulty and complexity of multi-objective optimization model, we transfer the problem in (45) into single-objective optimization by using weighting objectives method. In most realistic scenarios of vehicular network, the importance for two links sharing the same source is different. On the basis of conforming the generality, we denote the weighting factor as κ. Then the optimization model is converted into

$$\begin{aligned} &\max_{\varphi}\ [\kappa R_R(\varphi) + (1-\kappa)R_U(1-\varphi)] \\ &s.t.\ \varphi \in [0,1] \\ &\quad \kappa \in (0,1) \\ &\quad Pr_R(\varphi) \le p_R \\ &\quad Pr_U(1-\varphi) \le p_U. \end{aligned} \quad (46)$$

The scheme to optimize the transmit power so as to maximize the ergodic achievable rate guaranteeing the outage performance is shown in the *Algorithm* below. The complexity of this algorithm is $O(K)$ where K is the discrete dimension of φ. The complexity is determined by the discrete interval value, which is low for current well-developed communication systems.

V. PERFORMANCE EVALUATION

In this section, numerical simulations are provided under different settings to validate our results. In consideration of both generality and convenience, we analyze the urban macro cell scenario where the path-loss fading coefficient is set as $\alpha = 4$. We assume the reference distance to be in unity that $d_0 = 1$. We also set the noise variance as 1, and the SNR

Algorithm 1 Power allocation scheme to maximize ergodic achievable rate guaranteeing the outage performance requirements

Input a set of system parameters including the weighting factor κ, the channel parameters for each link, and the outage performance requirements, $R_{sum}^{\max} = 0$.
Output the ergodic achievable sum rate.
for each $\varphi = 0 : \Delta\varphi : 1$, **do**
  calculate the corresponding outage probability $\Pr_R$ and $\Pr_U$, respectively, based on the results in *Theorem 1*
  if $\Pr_R \leq p_R$ and $\Pr_U \leq p_U$, **then**
    calculate the corresponding ergodic achievable rate $R_{R,up}$ and $R_{U,up}$ respectively, based on (32)
    calculate the weighted ergodic achievable sum rate $R_{sum} = \kappa R_R(\varphi) + (1-\kappa) R_U(1-\varphi)$
    if $R_{sum} \geq R_{sum}^{\max}$, **then**
      $R_{sum}^{\max} \leftarrow R_{sum}$, $\varphi^{opt} \leftarrow \varphi$
    else if continue
    end if
  else if continue
  end if
end for

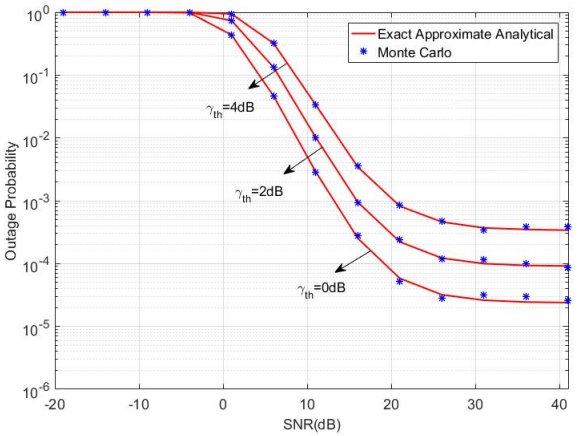

FIGURE 2. Comparison of exact analytical and Monte Carlo simulated results for outage probability.

at vehicles is formulated as SNR$= P_i/N_i$. All the Nakagami fading channels are independent and identically distributed. The Monte Carlo results are generated by averaging over 10^6 independent channel realisations. Although in our performance evaluation section, the results are obtained for some fixed fading scenarios, they are valid for an arbitrary fading scenario since we do not impose any specific constraint in our derivations.

Figure 2 verifies the validity of our analytical results for the outage performance in *Theorem 1*. We compare the exact analytical results with Monte-Carlo simulated results for different predetermined ratio γ_{th}. Here, we set $d_{1R} = 3$, $m_1 = 3$ and $m_2 = 2$. As anticipated, a perfect agreement is shown

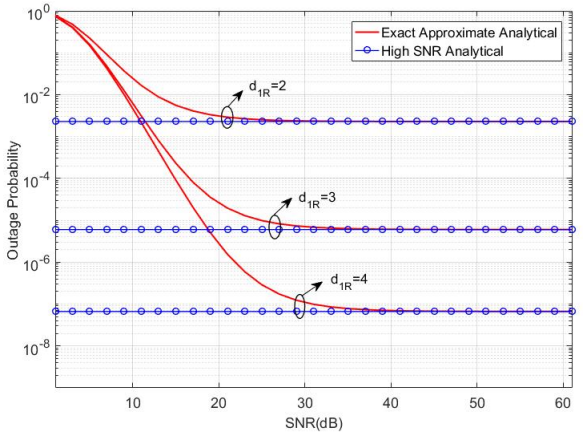

FIGURE 3. Comparison of exact analytical and high SNR analytical results for outage probability.

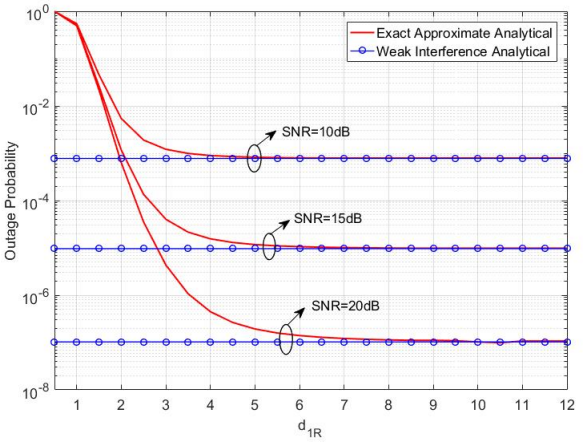

FIGURE 4. Comparison of exact analytical and weak interference analytical results for outage probability.

between the analytical and simulated curves for all the SNR regime.

We compare the exact analytical results of outage performance against the high SNR approximation in *Corollary 2*, for different levels of interference influenced by sharing the same time-frequency resources. In Fig. 3 we set $m_1 = 3$, $m_2 = 3$, $\gamma_{th} = 0dB$. As expected, the approximations for high SNR case seem to be noticeably tight even for moderate SNR range (e.g. approximately 30dB). We observe that a longer distance between two links reduces the interference at the receiver, thereby leading to a smaller outage probability. Moreover, the increasing SNR has a diminishing effect on the outage performance, which yields a certain value. That is, the results in *Corollary 2* can accurately predict the outage probability over a wide SNR regime.

In Fig. 4, the exact and weak interference approximate analytical results are provided against the distance between V_1 and V_R. We assume $m_1 = 4, m_2 = 3, and$ $\gamma_{th} = 0dB$. Different SNR curves are plotted in the figure (SNR$= 10, 15, 20dB$). Again, a precise agreement

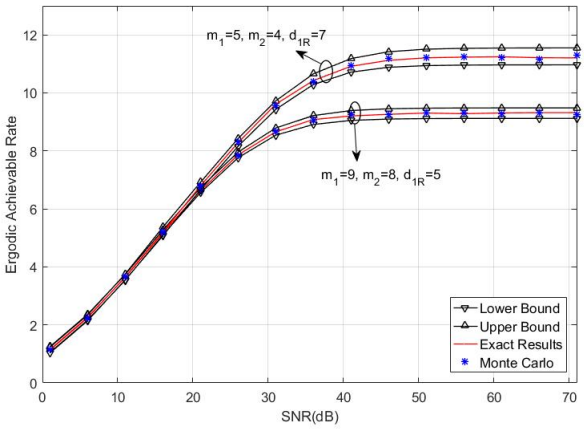

FIGURE 5. Comparison of exact analytical tight bounds, as well as Monte Carlo simulations for ergodic achievable rate.

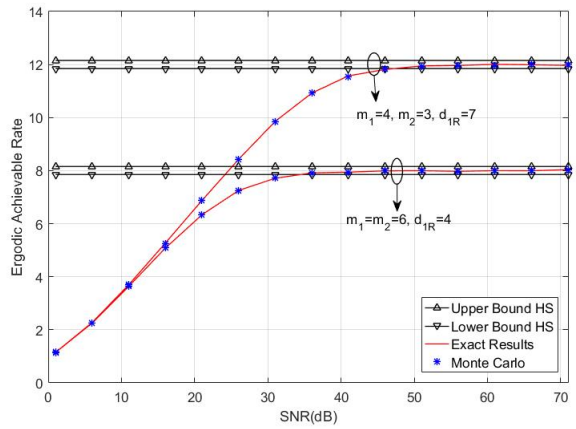

FIGURE 6. Comparison of exact analytical and high SNR analytical results for ergodic achievable rate.

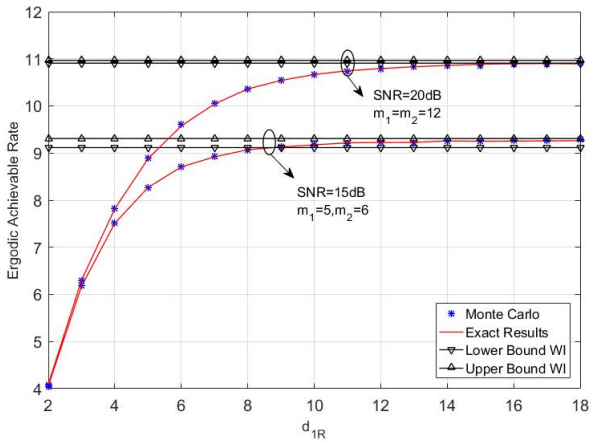

FIGURE 7. Comparison of exact analytical and weak interference analytical results for the bounds of ergodic achievable rate.

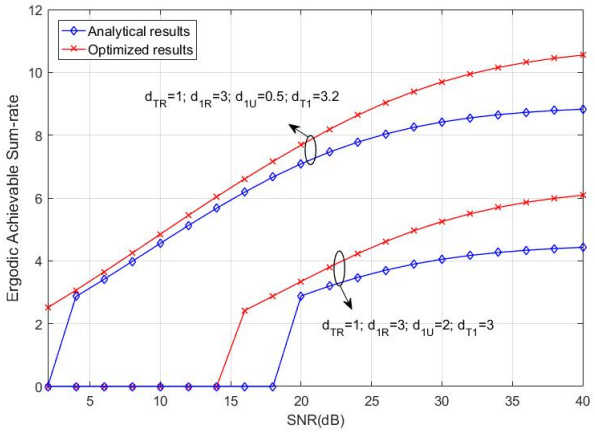

FIGURE 8. Comparison of proposed power allocation strategy and equal power strategy for the ergodic achievable sum-rate.

between exact and weak interference analytical results is seen in the figure. The weak interference approximations are shown to converge to their respective exact analytical results for medium and long d_{1R}. From Fig. 2- Fig. 4, this phenomena proves that our analytical results are tight for various tested topologies.

Figure 5 depicts the closed-form upper and lower bounds for the ergodic achievable rate based on *Theorem 2*, the exact analytical results in (30), as well as, Monte Carlo results. All the curves are presented as a function of SNR at transmitters. As anticipated, we clearly see that both upper and lower bound remain fairly close to the Monte Carlo simulated ergodic achievable rate for all the considered system configurations. More importantly, the upper bound almost coincides with the Monte Carlo results for low to middle SNR regime. The ergodic achievable remains robust to an increased SNR and all the curves converge to diverse certain values depending on the network parameters, for instance, the transmit power and the location of each node.

We now assess the proposed approximated high SNR bounds for ergodic achievable rate by setting $(m_1, m_2, d_{1R}) = ((6, 5, 7); (10, 10, 4))$ in Fig. 6. Here we evaluate the tightness of weak interference bounds $R^{HS}_{1R,lo}$ and $R^{HS}_{1R,up}$ in (36) and (37). From Fig. 6, the bounds in *Theorem 2* match accurately with Monte-Carlo results. We can find that when the SNR at the user increases, the SNR ceiling effect takes into effect at impractical SNR regime.

In Fig. 7, the simulated results along with the approximate weak interference bounds in *Corollary 5* are provided against the distance between two links. We assume $(m_1, m_2, SNR) = ((5, 6, 15); (18, 18, 20))$ in this figure. As anticipated, when the distance between two links increases, the interference level reduces. As d_{1R} is larger than a threshold, the ergodic achievable approaches to a certain value which is dominated without interference. Furthermore, it shows that the larger channel parameter m_1, m_2 can squeeze the gap between the lower and upper bounds which verifies the correctness of our analysis.

Figure 8 provides the ergodic achievable sum-rate against SNR under power allocation scheme in different parameter configurations. We also show the curves

under equal power case for comparison. Here, the location of each node is assumed as $(d_{TR}, d_{1R}, d_{1U}, d_{TU}) = ((0.5, 3, 1, 3.2); (1, 3, 2, 3))$. As expected, again, the ergodic achievable rate depends on the topologies of vehicular networks. From Fig. 8, performance of the proposed power allocation scheme significantly exceeds that of the equal allocation. It shows that the higher SNR at the transmitter achieves a more ergodic achievable rate compared to an equal case. This simulation result highlights the truth that the presented power allocation algorithm is particularly valid and effective for various locations of users, as well as, the noise. The power allocation scheme is proposed to maximize the ergodic achievable sum rate guaranteeing the outage probability of each link. In the low SNR regime, the outage probability falls below the threshold, and the communication link occur interrupt. Therefore, the ergodic achievable sum rate is reduced to zero.

VI. CONCLUSION

This paper have investigated the vehicular communications by sharing the common time-frequency resources in vehicular networks under Nakagami fading channels. We analyzed the outage probability, as well as the tight bounds of ergodic achievable rate, and provided the corresponding closed-form expressions. Two special scenarios, namely, high SNR case and weak interference case were discussed. For each scenario, the approximations were obtained with closed-form expressions, respectively. According to these results, several primary factors which play a destructive role for the network performance were revealed. Furthermore, the power allocation algorithm was provided to optimize the ergodic achievable rate at the same time guaranteeing the outage performance. All the results shown in this paper can be applied for arbitrary network topologies and system parameters. Numerical simulations validated our analytical results.

APPENDIX A
PROOF OF LEMMA 1

When $n_1 \leq n_2$, and we let $x \leftarrow x - \eta$, then we have

$$I(\mu, \eta, \xi; n_1, n_2) = exp(\mu\eta) \sum_{j=0}^{n_1} C_{n_1}^{j} (-\eta)^{n_1-j} \times \underbrace{\int_{\xi+\eta}^{+\infty} \frac{x^j \exp(-\mu x)}{x^{n_2}} dx}_{I_0}. \quad (47)$$

Since $j \leq n_1 \leq n_2$, the integral term I_0 is n-order exponential integral, (47) can be written as

$$I(\mu, \eta, \xi; n_1, n_2) = exp(\mu\eta) \sum_{j=0}^{n_1} C_{n_1}^{j} (-\eta)^{n_1-j} \int_{\xi+\eta}^{+\infty} \frac{\exp(-\mu x)}{x^{n_2-j}} dx \quad (48)$$

Let $t = x/(\xi + \eta)$, we get

$$I(\mu, \eta, \xi; n_1, n_2) = exp(\mu\eta) \sum_{j=0}^{n_1} C_{n_1}^{j} \frac{(-\eta)^{n_1-j}}{(\xi+\eta)^{n_2-j-1}} \times \int_{1}^{+\infty} \frac{\exp(-\mu(\xi+\eta)t)}{t^{n_2-j}} dt. \quad (49)$$

With the help of [[41], Eq.358], we can obtain

$$I(\mu, \eta, \xi; n_1, n_2) = exp(\mu\eta) \sum_{j=0}^{n_1} C_{n_1}^{j} \frac{(-\eta)^{n_1-j}}{(\xi+\eta)^{n_2-j-1}} \times E_{n_2-j}(\mu(\xi+\eta)). \quad (50)$$

When $n_1 > n_2$, for the case $j \leq n_2$, it converts into the problem in (47). For the case $n_2 \leq j \leq n_1$, the integral term I_0 can be expressed by

$$\begin{aligned} &I(\mu, \eta, \xi; n_1, n_2) \\ &= \underbrace{exp(\mu\eta) \sum_{j=0}^{n_2} C_{n_1}^{j} (-\eta)^{n_1-j} \int_{\xi+\eta}^{+\infty} \frac{\exp(-\mu x)}{x^{n_2-j}} dx}_{I^{(a)}(\mu,\eta,\xi;n_1,n_2)} \\ &\quad + \underbrace{exp(\mu\eta) \sum_{j=n_2+1}^{n_1} C_{n_1}^{j} (-\eta)^{n_1-j} \int_{\xi+\eta}^{+\infty} x^{j-n_2} \exp(-\mu x) dx}_{I^{(b)}(\mu,\eta,\xi;n_1,n_2)} \end{aligned} \quad (51)$$

where $I^{(a)}(\mu, \eta, \xi; n_1, n_2)$ can be easily obtained with the analysis for the case $n_1 \leq n_2$. Now we focus on $I^{(b)}(\mu, \eta, \xi; n_1, n_2)$, we have

$$I^{(b)}(\mu, \eta, \xi; n_1, n_2) = exp(\mu\eta) \sum_{j=n_2+1}^{n_1} C_{n_1}^{j} (-\eta)^{n_1-j} \times \underbrace{\int_{\xi+\eta}^{+\infty} x^{j-n_2} \exp(-\mu x) dx}_{I_0^{(b)}}. \quad (52)$$

With the help of [[41] Eq.(3.151.2)], the integrals in (52) can be obtained as

$$I_0^{(b)} = \mu^{n_2-j-1} \Gamma(j - n_2 + 1, \mu(\xi+\eta)) \quad (53)$$

where $\Gamma(n, z)$, $n \in N^*, z > 0$ is upper incomplete gamma function defined as

$$\Gamma(n, z) = \exp(z) \sum_{k=0}^{n-1} \frac{(n-1)!}{k!} z^k. \quad (54)$$

Submitting (53) into (52), we can easily obtain the expression for $I^{(b)}(\mu, \eta, \xi; n_1, n_2)$. Based on the above results, we arrive at the expressions for $I(\mu, \eta, \xi; n_1, n_2)$ in *Lemma 1*.

APPENDIX B
PROOF OF THEOREM 2

Based on the well-know Jensen's inequality

$$\log_2\left(1+\frac{1}{E\left[1/\gamma_R\right]}\right) \le E\left[\log_2\left(1+\gamma_R\right)\right] \le \log_2\left(1+E\left[\gamma_R\right]\right) \quad (55)$$

we now derive the expressions for $E\left[1/\gamma_R\right]$ and $E\left[\gamma_R\right]$ respectively. According to the pdf of γ_R in (18), we have

$$E\left[1/\gamma_R\right] = \int_0^{+\infty} \frac{1}{w} \times f_{\gamma_R}(w)\, dw. \quad (56)$$

After some basic algebraic manipulations, it yields

$$E\left[1/\gamma_R\right] = \prod_{l=1}^{2}\left(\frac{m_l}{\sigma_l\Omega_l}\right)^{m_l}\frac{1}{\Gamma(m_l)} \times \sum_{i=0}^{m_1} C_m^i N_0^{m-i}\left(\frac{\Omega_1\sigma_1}{m_1}\right)^{m_2+i}\Gamma(m_2+i) \times \int_0^{+\infty}\frac{w^{m_1-2}}{(w+\tau)^{m_2+i}}\exp\left(-\frac{m_1N_0w}{\Omega_1\sigma_1}\right)dw. \quad (57)$$

Utilizing the results in *Lemma 1*, (57) can be transformed into

$$E[1/\gamma_R] = \prod_{l=1}^{2}\left(\frac{m_l}{\sigma_l\Omega_l}\right)^{m_l}\frac{1}{\Gamma(m_l)} \times \sum_{i=0}^{m_1} C_m^i N_0^{m-i}\left(\frac{\Omega_1\sigma_1}{m_1}\right)^{m_2+i}\Gamma(m_2+i) \times I\left(\frac{m_1N_0}{\Omega_1\sigma_1}, \frac{m_2\Omega_1\sigma_1}{m_1\Omega_2\sigma_2}, 0; m_1-2, m_2+i\right). \quad (58)$$

Similarly, we give the expression for $E\left[\gamma_R\right]$ as follows

$$E[\gamma_R] = \prod_{l=1}^{2}\left(\frac{m_l}{\sigma_l\Omega_l}\right)^{m_l}\frac{1}{\Gamma(m_l)} \times \sum_{i=0}^{m_1} C_m^i N_0^{m-i}\left(\frac{\Omega_1\sigma_1}{m_1}\right)^{m_2+i}\Gamma(m_2+i) \times I\left(\frac{m_1N_0}{\Omega_1\sigma_1}, \frac{m_2\Omega_1\sigma_1}{m_1\Omega_2\sigma_2}, 0; m_1, m_2+i\right). \quad (59)$$

Having the above results and combining them with (31), we arrive at the results in *Theorem 2*.

REFERENCES

[1] F. J. Martinez, C.-K. Toh, J.-C. Cano, C. T. Calafate, and P. Manzoni, "Emergency services in future intelligent transportation systems based on vehicular communication networks," *IEEE Intell. Transp. Syst. Mag.*, vol. 2, no. 2, pp. 6–20, Oct. 2010.

[2] *Annual Global Road Crash Statistics*. Accessed: Dec. 15, 2019. [Online]. Available: http://asirt.org/initiatives/informing-road-users/road-safety-facts/road-crash-statistics

[3] Y. Li, X. Zhu, D. Jin, and D. Wu, "Multiple content dissemination in roadside-unit-aided vehicular opportunistic networks," *IEEE Trans. Veh. Technol.*, vol. 63, no. 8, pp. 3947–3956, Oct. 2014.

[4] S. Al-Sultan, M. M. Al-Doori, A. H. Al-Bayatti, and H. Zedan, "A comprehensive survey on vehicular ad hoc network," *J. Netw. Comput. Appl.*, vol. 37, pp. 380–392, Jan. 2014.

[5] N. Lu, N. Cheng, N. Zhang, X. Shen, and J. W. Mark, "Connected vehicles: Solutions and challenges," *IEEE Internet Things J.*, vol. 1, no. 4, pp. 289–299, Aug. 2014.

[6] J. B. Kenney, "Dedicated short-range communications (DSRC) standards in the United States," *Proc. IEEE*, vol. 99, no. 7, pp. 1162–1182, Jul. 2011.

[7] J. N. G. Isento, J. J. P. C. Rodrigues, J. A. F. F. Dias, M. C. G. Paula, and A. Vinel, "Vehicular delay-tolerant networks A novel solution for vehicular communications," *IEEE Intell. Transp. Syst. Mag.*, vol. 99, no. 7, pp. 1162–1182, Jul. 2011.

[8] L. Liang, H. Peng, G. Y. Li, and X. Shen, "Vehicular communications: A physical layer perspective," *IEEE Trans. Veh. Technol.*, vol. 66, no. 12, pp. 10647–10659, Dec. 2017.

[9] H. Peng, L. Liang, X. Shen, and G. Y. Li, "Vehicular communications: A network layer perspective," *IEEE Trans. Veh. Technol.*, vol. 68, no. 2, pp. 1064–1078, Feb. 2019.

[10] J. Mei, K. Zheng, L. Zhao, L. Lei, and X. Wang, "Joint radio resource allocation and control for vehicle platooning in LTE-V2V network," *IEEE Trans. Veh. Technol.*, vol. 67, no. 12, pp. 12218–12230, Dec. 2018.

[11] X. Zhang, Y. Shang, X. Li, and J. Fang, "Research on overlay D2D resource scheduling algorithms for V2V broadcast service," in *Proc. IEEE VTC-Fall*, Sep. 2016, pp. 1–5.

[12] S. Park, B. Kim, H. Yoon, and S. Choi, "RA-eV2V: Relaying systems for LTE-V2V communications," *J. Commun. Netw.*, vol. 20, no. 4, pp. 396–405, Aug. 2018.

[13] Y. Xu and X. Gu, "Resource allocation for NOMA-based V2V system," in *Proc. IC-NIDC*, Aug. 2018, pp. 239–243.

[14] B. Li, D. He, Y. Feng, Y. Xu, and H. Zheng, "Spectrum resource allocation scheme for alarm information delivery in V2V communication," in *Proc. IEEE VTC-Fall*, Aug. 2018, pp. 1–5.

[15] C. Guo, L. Liang, and G. Y. Li, "Resource allocation for vehicular communications with low latency and high reliability," *IEEE Trans. Wireless Commun.*, vol. 18, no. 8, pp. 3887–3902, Aug. 2019.

[16] R. Woo, D. S. Han, and J.-H. Song, "Performance analysis for priority based broadcast in vehicular networks," in *Proc. ICUFN*, Jul. 2013, pp. 51–55.

[17] Y. Yao, L. Rao, and X. Liu, "Performance and reliability analysis of IEEE 802.11p safety communication in a highway environment," *IEEE Trans. Veh. Technol.*, vol. 62, no. 9, pp. 4198–4212, Nov. 2013.

[18] N. Cheng, H. Zhou, L. Lei, N. Zhang, Y. Zhou, X. Shen, and F. Bai, "Performance analysis of vehicular Device-to-Device underlay communication," *IEEE Trans. Veh. Technol.*, vol. 66, no. 6, pp. 5409–5421, Jun. 2017.

[19] A. Bazzi, B. M. Masini, and A. Zanella, "Performance analysis of V2V beaconing using LTE in direct mode with full duplex radios," *IEEE Wireless Commun. Lett.*, vol. 4, no. 6, pp. 685–688, Dec. 2015.

[20] M. Nithya and G. Ananthi, "Performance analysis of vehicular ad-hoc networks with space shift keying modulation," in *Proc. WiSPNET*, Mar. 2017, pp. 1951–1954.

[21] Q. Zheng, K. Zheng, L. Sun, and V. C. M. Leung, "Dynamic performance analysis of uplink transmission in cluster-based heterogeneous vehicular networks," *IEEE Trans. Veh. Technol.*, vol. 64, no. 12, pp. 5584–5595, Dec. 2015.

[22] M. Noor-A-Rahim, G. G. M. N. Ali, Y. L. Guan, B. Ayalew, P. H. J. Chong, and D. Pesch, "Broadcast performance analysis and improvements of the LTE-V2V autonomous mode at road intersection," *IEEE Trans. Veh. Technol.*, vol. 68, no. 10, pp. 9359–9369, Oct. 2019.

[23] X. Ge, H. Cheng, G. Mao, Y. Yang, and S. Tu, "Vehicular communications for 5G cooperative small-cell networks," *IEEE Trans. Veh. Technol.*, vol. 65, no. 10, pp. 7882–7894, Oct. 2016.

[24] J. Chen, G. Mao, C. Li, A. Zafar, and A. Y. Zomaya, "Throughput of infrastructure-based cooperative vehicular networks," *IEEE Trans. Intell. Transp. Syst.*, vol. 18, no. 11, pp. 2964–2979, Nov. 2017.

[25] K. Eshteiwi, G. Kaddoum, K. Ben Fredj, E. Soujeri, and F. Gagnon, "Performance analysis of full-duplex vehicle relay-based selection in dense multi-lane highways," *IEEE Access*, vol. 7, pp. 61581–61595, 2019.

[26] X. Li, J. Li, and L. Li, "Performance analysis of impaired SWIPT NOMA relaying networks over imperfect Weibull channels," *IEEE Syst. J.*, vol. 14, no. 1, pp. 669–672, Mar. 2020.

[27] S. Ö. Ata and İ. Altunbaş, "Fixed-gain AF PLNC over cascaded Nakagami-*m* fading channels for vehicular communications," *AEU-Int. J. Electron. Commun.*, vol. 70, no. 4, pp. 510–516, 2016.

[28] R. Chen, Z. Sheng, Z. Zhong, M. Ni, V. C. M. Leung, D. G. Michelson, and M. Hu, "Connectivity analysis for cooperative vehicular ad hoc networks under Nakagami fading channel," *IEEE Commun. Lett.*, vol. 18, no. 10, pp. 1787–1790, Oct. 2014.

[29] M. M. Ninsi and P. C. Neelakantan, "Analyzing the network connectivity probability of a linear VANET in Nakagami fading channels," in *Proc. ICDCN*, 2014, pp. 505–511.

[30] H. Ilhan, "Performance analysis of two-way AF relaying systems over cascaded Nakagami-*m* fading channels," *IEEE Signal Process. Lett.*, vol. 19, no. 6, pp. 332–335, Jun. 2012.
[31] G. C. Alexandropoulos, A. Papadogiannis, and K. Berberidis, "Performance analysis of cooperative networks with relay selection over Nakagami-*m* fading channels," *IEEE Signal Process. Lett.*, vol. 17, no. 5, pp. 441–444, May 2010.
[32] P.-T. Van, H.-H. Nguyen Le, M.-D. Nguyen Le, and D.-B. Ha, "Performance analysis in wireless power transfer system over Nakagami fading channels," in *Proc. ICEIC*, Jan. 2016, pp. 1–4.
[33] R. Zhao and L. Yang, "Performance analysis of fixed gain relaying systems in Nakagami-*m* fading channels," in *Proc. WCSP*, Nov. 2009, pp. 1–5.
[34] B. Maham and A. Hjorungnes, "Asymptotic performance analysis of amplify-and-forward cooperative networks in a Nakagami-*m* fading environment," *IEEE Commun. Lett.*, vol. 13, no. 5, pp. 300–302, May 2009.
[35] A. A. Hassan, L. H. Afify, A. A. El-Sherif, and T. Elbatt, "Impact of temporally correlated Nakagami-*m* interferers in D2D cache-aided networks," in *Proc. IEEE WCNC*, Apr. 2019, pp. 1–6.
[36] S. Das, "Performance analysis of OFDM based decode-and-forward relay over Nakagami fading channel," in *Proc. ICEEICT*, Apr. 2014, pp. 1–4.
[37] X. Li, M. Zhao, C. Zhang, W. U. Khan, J. Wu, K. M. Rabie, and R. Kharel, "Security analysis of multi-antenna NOMA networks under I/Q imbalance," *Electronics*, vol. 8, no. 11, p. 1327, Nov. 2019.
[38] X. Li, Q. Wang, H. Peng, H. Zhang, D.-T. Do, K. M. Rabie, R. Kharel, and C. C. Cavalcante, "A unified framework for HS-UAV NOMA networks: Performance analysis and location optimization," *IEEE Access*, vol. 8, pp. 13329–13340, 2020.
[39] X. W. Li, J. J. Li, Y. W. Liu, Z. G. Ding, and A. Nallanathan, "Residual transceiver hardware impairments on cooperative NOMA networks," *IEEE Trans. Wireless Commun.*, vol. 19, no. 1, pp. 680–695, Jan. 2020.
[40] X. Yue and Y. Liu, "Performance analysis of intelligent reflecting surface assisted NOMA networks," 2020, *arXiv:2002.09907*. [Online]. Available: http://arxiv.org/abs/2002.09907
[41] I. S. Gradshteyn and I. M. Ryzhik, *Table of Integrals, Series, and Products*, 7th ed. San Diego, CA, USA: Academic, 2007.
[42] B. Lu, S. Lin, J. Shi, and Y. Wang, "Resource allocation for D2D communications underlaying cellular networks over Nakagami-*m* fading channel," *IEEE Access*, vol. 7, pp. 21816–21825, 2019.

YIYANG NI (Member, IEEE) received the B.S. degree in communications engineering and the Ph.D. degree from the Nanjing University of Posts and Telecommunications (NJUPT), Nanjing, China, in 2008 and 2016, respectively.

She is currently holding the postdoctoral position in electronic science and technology with NJUPT. She is also an Associate Professor with Jiangsu Second Normal University. She is also with the Jiangsu Institute of Educational Science Research. Her research interests include wireless communications and the Internet of Things.

YAXUAN LIU (Graduate Student Member, IEEE) is currently pursuing the B.S. degree with Jiangsu Second Normal University, Nanjing, China. Her research interests include wireless communications and the Internet of Things.

QIN WANG (Member, IEEE) received the B.S. degree in communications engineering and the Ph.D. degree in communication and information system from the Nanjing University of Posts and Telecommunications (NJUPT), China, in 2011 and 2016, respectively. From 2015 to 2016, she was a Visiting Scholar with the Department of Computer Science, San Diego State University, USA. She is currently holding the postdoctoral position in electronic science and technology with NJUPT. She is also an Assistant Professor with the College of Engineering and Computing Sciences, New York Institute of Technology (NYIT), Nanjing. Her research interests include multimedia communications, multimedia pricing, resource allocation in 5G, and the Internet of Things. She serves as a Technical Program Committee Member for many international conferences, such as ICC 2018, ICNC 2018, and CCNC 2017. She serves as a Track Co-Chair for MIPR 2019. She serves as a Reviewer for many journals, such as the IEEE TRANSACTIONS ON WIRELESS COMMUNICATIONS and the IEEE TRANSACTIONS ON VEHICULAR TECHNOLOGY. She serves as a Co-Editor for the *IoT Journal* (Elsevier).

YUXI WANG received the B.S. degree in computer science and technology from Nanjing Normal University, Nanjing, China, in 2001, and the M.S. degree in computer technology from the Nanjing University of Aeronautics and Astronautics, Nanjing, in 2009. He is currently an Associate Professor with the College of Mathematics and Information Technology, Jiangsu Second Normal University. His research interests include wireless sensor networks and wireless communications.

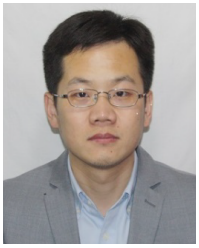

HAITAO ZHAO (Member, IEEE) received the M.S. degree and the Ph.D. degree (Hons.) in signal and information processing from the Nanjing University of Posts and Telecommunications, Nanjing, China, in 2008 and 2011, respectively. He is currently an Associate Professor with the Nanjing University of Posts and Telecommunications. His current research interests include wireless multimedia modeling, capacity prediction, and wireless network coding.

HONGBO ZHU (Member, IEEE) received the B.S. degree in communications engineering from the Nanjing University of Posts and Telecommunications, Nanjing, China, in 1982, and the Ph.D. degree in information and communications engineering from the Beijing University of Posts and Telecommunications, Beijing, China, in 1996. He is currently a Professor with the Nanjing University of Posts and Telecommunications. He is also the Head of the Coordination Innovative Center of the Internet of Things (IoT) Technology and Application, Jiangsu, which is the first governmental authorized Coordination Innovative Center of the IoT in China. He is also leading a big group and multiple funds on the IoT and wireless communications with current focus on architecture and enabling technologies for the IoT. He also serves as a referee or an expert in multiple national organizations and committees. He has authored or coauthored over 200 technical papers published in various journals and conferences. His research interests include mobile communications, wireless communication theory, and electromagnetic compatibility.